RES MILITARIS
REVUE EUROPEENNE D ETUDES EUROPEAN JOURNAL OF MILITARY STUDIES
Social Science Journal

An analysis of a car radiator's thermal performance using Cu_2O_3- Ethylene Propylene + Water Based Nanofluids

M.Venkatesan[1], M.Dinesh Kumar[2], N.Prithiviraj[3], S.Saravana Kumar[4]

[1,2,3,4] Assistant Professor,
Department of Mechanical Engineering,
Excel Engineering College, Komarapalayam - 637307, Tamil Nadu, India.

Abstract

This investigation meticulously examined the thermal transfer capabilities of nanofluids, specifically a suspension of Cu2O3 nanoparticles in a volumetric mixture of 70:30 Propylene Glycol and water, in comparison to the base fluid. The analysis was conducted by modelling the flow dynamics within both laminar and turbulent flow regimes in a flat tube representative of a radiator, utilizing both single-phase and Eulerian-Eulerian multiphase methodologies within computational fluid dynamics (CFD) simulation frameworks. The Nusselt number was determined by varying the Reynolds number across both models, subsequently comparing the results with established theoretical correlations and the empirical data documented in existing literature. The influence of alterations in volumetric concentrations, inlet velocities, inlet temperatures, and nanoparticle sizes on the thermal transfer performance metrics of nanofluids was rigorously assessed. The multiphase modelling approach demonstrated a more pronounced enhancement in the Nusselt number compared to the single-phase approach at equivalent volume fractions. Furthermore, the multiphase model illustrated that the Nusselt number exhibits an increase up to a specific threshold with rising volume fractions, beyond which additional increases in volume fraction do not yield any substantial enhancement. As the Reynolds number increased, both the Nusselt number and the surface heat transfer coefficient exhibited an upward trend for both laminar and turbulent flow conditions. Additionally, the skin friction coefficient, pressure drop across the inlet and outlet, and the necessary

pumping power exhibited a slight increase in response to elevated volume fractions. Notably, variations in nanoparticle size indicated that optimal performance was achieved at a nanoparticle size of 25 nm.

Keywords: Nanofluid, Cu2O3, Flat tube, CFD, Car radiator

1. Introduction

Automotive radiators serve as cross-flow heat exchangers integral to the engine cooling system. Currently, both conduction and convection mechanisms are employed within automotive cooling systems to effectively dissipate the surplus heat generated from the incessant functioning of the engine, where radiators utilize water in conjunction with an antifreeze agent as coolant [1]. Nonetheless, the prevailing methods for heat extraction from engines exhibit inefficiencies that hinder their ability to adequately eliminate excess thermal energy. In contemporary contexts, industries demonstrate an increasing emphasis on enhancing fuel efficiency while simultaneously reducing the complexities associated with radiator functionalities. As articulated by Bergles et al., the paramount thermal-hydraulic objectives within heat exchanger apparatuses include a reduction in the dimensions of the heat exchanger required for a specific heat duty (capacity), enhancement of the performance and operational capabilities of existing heat exchangers, and a decrease in the power required for pumping [2]. Consequently, investigations aimed at identifying innovative or refined approaches to augment the overall efficiency of automotive radiator systems have garnered significant traction over the years. Diverse models of heat exchangers, characterized by various fin designs and tube configurations, have been integrated to enhance radiator capacity and design compactness, thereby striving to maximize their efficiency.

A research endeavour conducted by Ali et al. indicated that the conventional modifications of radiator fins and micro-channels aimed at augmenting the cooling efficacy have reached their respective limits [3]. However, it is noteworthy that the types of fluids utilized within heat exchangers have predominantly remained unchanged. The suboptimal heat transfer characteristics of traditional coolant fluids have spurred contemporary researchers to explore advanced technologies and alternative fluids capable of improving the thermal transfer rates and associated properties of the fluid, thereby enhancing the cooling performance of automotive radiators. The recent advancements in nanotechnology have facilitated substantial progress in this realm of research.

Choi and Eastman introduced the paradigm of "Nano Fluid" in 1995, endeavouring to enhance the thermal transfer characteristics of conventional fluids [4]. Nanofluids are defined as dispersions of nanoparticles, typically in the nanometer size range, which include metals, metal oxides, and nanostructured carbon compounds (such as graphene and carbon nanotubes), within traditional fluids. Recent investigations have demonstrated that nanofluids exhibit superior thermo-physical properties, including viscosity, thermal diffusivity, thermal conductivity, and surface heat transfer coefficients, when juxtaposed with commonly utilized base fluids such as oil or water [5]. Furthermore, they possess the potential to decrease energy consumption within heat exchangers for equivalent outputs, enhance the cooling rates of vehicles and heavy-duty engines, diminish the weight and complexity of thermal management systems, and ultimately reduce the manufacturing costs associated with automotive production [6].

Chandrasekar et al. [7] executed an experimental evaluation and scrutinized the performance of circular pipes utilizing alumina nanofluids, reporting an enhancement in the Nusselt Number,

relative to the base fluid, ranging from 15 to 21 percent through the application of nanofluids.

Peyghambarzadeh et al. [8] investigated the effects of employing Cu2O3-water nanofluids and observed a 40% increase in heat transfer relative to the base fluid (water) with augmentations in both the Reynolds number and the volume fraction of nanoparticles incorporated in the base fluid.

Shafahi et al. [9] utilized cylindrical-shaped heat pipes to conduct a two-dimensional Computational Fluid Dynamics (CFD) analysis employing nanofluids based on CuO, Cu2O3, and TiO2 nanoparticles. They reported that an increase in nanoparticle concentration significantly improved the thermal efficiency of the nanofluids.

Vajjha et al. [10] conducted CFD analysis utilizing a single-phase methodology and incorporated silicon dioxide, copper oxide, and aluminum oxide as nanoparticles. Their findings indicated that CuO-based nanofluids yielded the highest heat transfer coefficients, while the pressure losses were maximized at the highest volume concentrations of any nanofluids employed. The friction factor was also observed to be the greatest in CuO-based nanofluids at equivalent volume fractions, inlet velocities, and temperatures.

Keshavarz et al. [11] performed CFD analysis by modeling the laminar flow of nanofluids under the assumption of constant heat flux through the tube wall, wherein the fluid flow exists within a fully developed region of circular cross-section tubes. By employing nanoparticles of 45 nm and 150 nm diameters at varying concentrations of 1%, 3%, 4%, and 6%, single-phase simulations were executed. A comparison with experimental data indicated discrepancies of up to 10% in heat transfer rates; it was observed that an elevation in nanoparticle concentration resulted in an increase of up to 9% in the convective heat transfer coefficient when contrasted with water as the base fluid.

Vajjha et al. [12] utilized a single-phase approach to model nanofluids in a mixture of Propylene Glycol and water as the base fluid within a flat tube of a car radiator. The computational results demonstrated an increase in both heat transfer coefficients and friction factors as the volume concentration of particles rose. It was concluded that for equivalent pumping power, CuO and Cu2O3 nanofluids at volumetric concentrations of up to 3% and 5% respectively exhibited enhanced thermodynamic parameters, such as heat transfer coefficients, in comparison to the base fluid. Zhao et al. [13] conducted numerical assessments in a flat tube using nanofluids and corroborated that both pressure drop and relative convective heat transfer were enhanced through the application of nanofluids.

In the multiphase modeling approach, the nanoparticles and the base fluid are regarded as two distinct phases, with mass, energy, and momentum equations being solved individually for both models while the interaction between the two phases is governed by various governing equations. The heat transfer characteristics of nanofluids in micro-channels under laminar flow conditions with a constant temperature were simulated by Kalteh et al. [14]. They employed a multiphase Eulerian-Eulerian approach to model the flow of nanofluids throughout the entire channel. The results from the two-phase simulation indicated a superior rate of heat transfer compared to those derived from the homogeneous model of the single-phase approach. In other terms, the Nusselt number values obtained from the single-phase model were observed to be 55% - 70% lower than those derived from the two-phase model results.

Delvari et al. [5] utilized both single-phase and multiphase methodologies to assess the heat transfer potential of Cu2O3 and CuO nanofluids, employing pure water and pure Propylene Glycol as base

fluids. They juxtaposed the outcomes from their numerical study with available experimental data, concluding that the multiphase model provided a more accurate prediction of the N.

2. Material and Methods:

A multitude of research endeavors have been conducted utilizing a single-phase methodology in the circular correction of a tube. Nevertheless, only a limited number of researchers have engaged in simulations employing the multiphase approach within a flat tube of a radiator, primarily due to the complexities associated with establishing multiphase models in Computational Fluid Dynamics (CFD) that can reliably forecast the interactions between two phases; both investigations demonstrated that the multiphase model provided superior predictions regarding the heat transfer capabilities of nanofluids. Both analyses were executed utilizing either pure Propylene Glycol or pure water as the foundational fluid. However, in the context of radiators, a mixture of Propylene Glycol and water (typically in a 70:30 volume/volume ratio) is commonly utilized. Consequently, this study adopts the Eulerian- Eulerian multiphase approach.

Table 1: Nusselt number from single-phase simulation and literature-available reference data are compared

Re	Nusselt Number (Single-phase)	Nusselt Number (Dittus-Boelter)	% Difference	Nusselt Number (Vajjha et al.)	% Difference
655	10	7.69	3.91	7.28	9.86
1327	15	13.44	-3.34	12.74	2.01
2000	21	18.63	-3.39	17.66	1.90
2672	24	23.46	-6.2	22.25	-1.13
3344	28	28.06	-7.34	26.61	-2.30

Table 2: Nusselt number from multiphase simulation and literature-available reference data are compared

Re	Nusselt Number (Multiphase)	Nusselt Number (Dittus and Boelter)	% Difference	Nusselt Number (Vajjha et al.)	% Difference
1002.63	8.13	8.76	7.53	8.42	10.51
2015.13	15.65	24.43	-9.5	15.85	-6.25
3028.25	20.16	29.65	-4.26	23.12	-1.32
3852.12	22.16	23.53	5.48	23.18	8.35
6012.35	24.26	32.53	16.75	29.86	18.18

3. Temperature variation along the tube

When the nanofluid is introduced through the inlet at an elevated temperature, thermal energy is dissipated to the ambient environment via the fins. As the fluid undergoes thermal loss, its temperature systematically declines from the inlet to the outlet. Figure 7 illustrates the reduction in temperature from 363 K at the tube's inlet to approximately 352 K at its outlet.

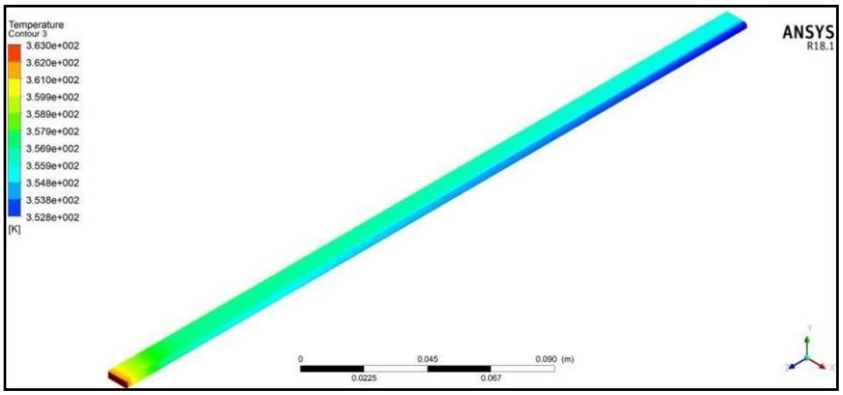

Figure 1: temperature profile throughout the tube at an input velocity of 0.3 m/s and a volume

fraction of 5%

As depicted in figure 8, the thermal characteristics of the fluid exhibit a lower temperature within the circular segments in comparison to the planar segments of the tube, attributable to the enhanced surface area present in the circular sections. Furthermore, the temperature profile illustrated in figure 8 indicates that the temperature reaches a minimum in proximity to the wall, which consists of a 0.0001m thick conductive layer made of Aluminium that constitutes the tube's covering. The thermal measurement approximates 360K within the central regions of the tube at the outlet section. Conversely, along the x-direction, the temperature diminishes to approximately 353K at the curved section of the tube. The relatively low temperatures observed in the peripheral regions of the tube, particularly adjacent to the curved wall, can be ascribed to the significantly higher surface heat transfer rates of 206 W/m²K to the ambient environment, overshadowing the conduction phenomenon enabled by the emergence of secondary flows and the exchange of turbulent kinetic energy, as evidenced in figures 9 and 10.

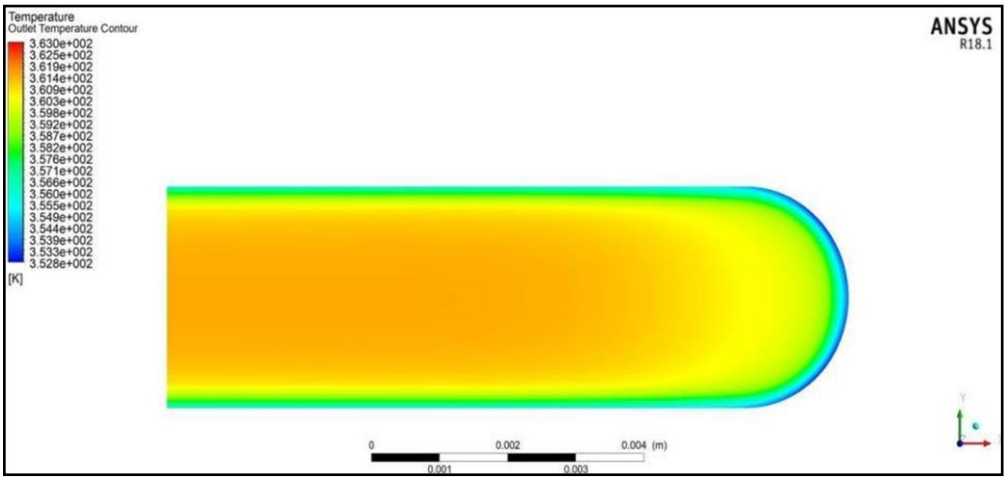

Figure 2: temperature contour at the outflow at an input velocity of 0.3 m/s and a volume percent of 5%

3.1. Y-velocity profile and Turbulent Kinetic Energy

The hydrodynamic behavior of fluid flow within a planar tube was systematically examined by segmenting it into two distinct regions; the initial region corresponds to the planar section of the tube wall, while the subsequent region pertains to the semi-circular section. Within the planar section, the fluid's velocity remains relatively consistent, whereas in the semi-circular area, the fluid velocity exhibits a pronounced decline, a phenomenon that is illustrated in figure 11b.

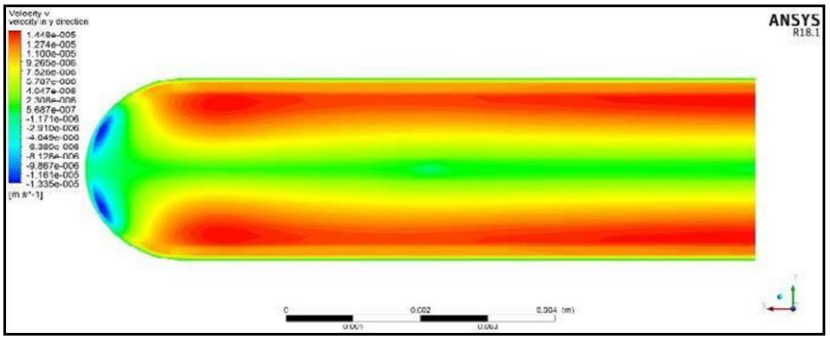

Figure 3: Fluid velocity contour in the Y direction at the outflow for a volume fraction of 5% and an inlet velocity of 0.3 m/s

Furthermore, the fluid's velocity in the y-direction is comparatively diminished in the curved segment relative to the flat segment of the tube, as evidenced in figure 9. This phenomenon can be attributed to the semi-circular segment facilitating the development of turbulent secondary flows, which is depicted in the velocity contour in the y-direction in figure 9, alongside figure 10 portraying the turbulence kinetic energy at the outlet. The semi-circular segment engenders a greater magnitude of secondary flows than the flat segment; consequently, the velocity diminishes as the fluid progresses toward the wall and ultimately reaches a state of zero.

The emergence of secondary flows, coupled with the attenuation of both axial and radial

velocities within the semi-circular segment, ultimately leads to a reduction in turbulence kinetic

energy, which consistently declines as one transitions from the flat segment to the curved semi-circular segment in a uniform manner.

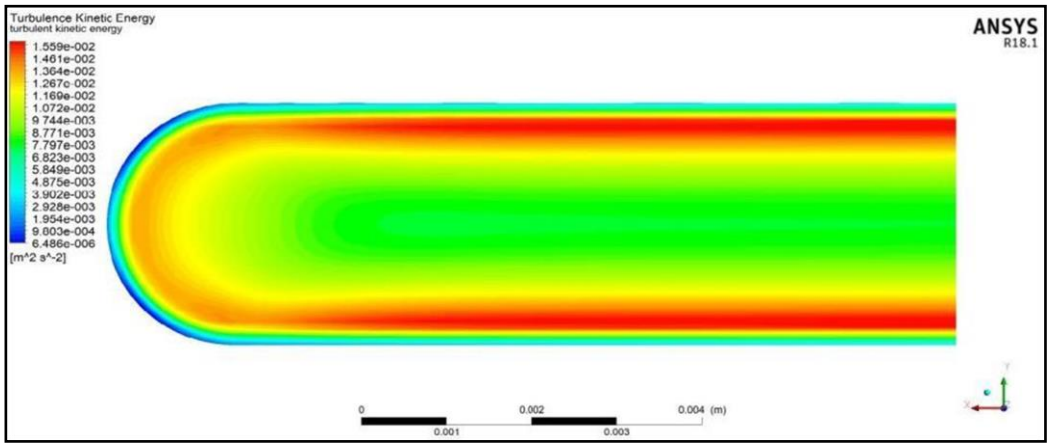

Figure 4: Fluid turbulence kinetic energy at the output at a volume percentage of 5% and an input velocity of 0.3 m/s

The reduction in velocity, along with the associated turbulence kinetic energy, diminishes the fluid mixing within the semi-circular region; consequently, there is a progressive decline in the surface heat transfer coefficient attributable to convection, as illustrated in figure 10a. Within the planar region, the surface heat transfer coefficient exhibits a nearly uniform distribution. In the curved region, a reduction is initiated, and there is a notable non-uniformity in the surface heat transfer coefficient at elevated velocities, which is a result of the increased turbulence observed at higher Reynolds numbers.

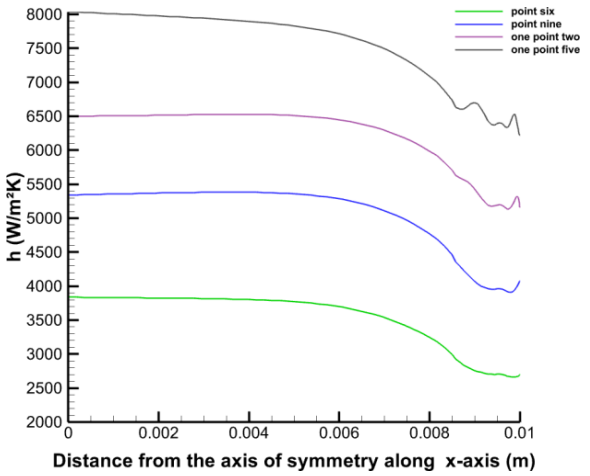

a. Variation in the coefficient of heat transfer

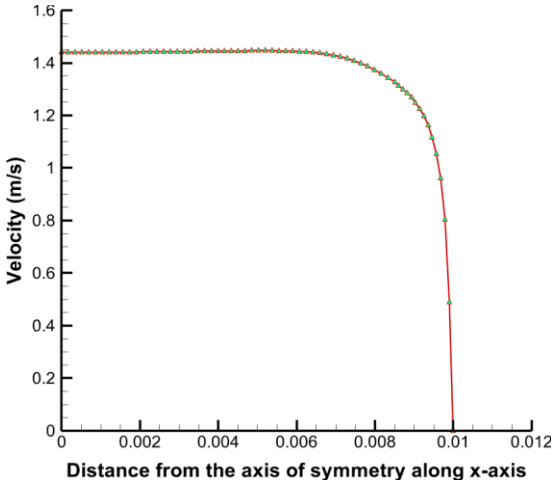

b. Variation in speed

Figure 5: Variation in the tube profile's x-axis surface heat transfer coefficient and velocity

3.2 Effect of Reynolds number

The Reynolds number was manipulated by adjusting the inlet velocity of the nanofluids within the range of 0.3 m/s to 1.5 m/s, while maintaining a constant volume fraction of 5% and a particle size of 25 nm, under an inlet temperature of 90°C. The influence on the Nusselt number and the surface heat transfer coefficient was examined through both single-phase and multiphase methodologies, and the computational findings were juxtaposed with the previously established experimental results obtained by a multitude of researchers.

3.3 Effect on Nusselt Number

For both single-phase and multiphase methodologies, the Nusselt number exhibited an increase corresponding to the progression of the Reynolds number from 1000 to 5500. As illustrated in

Figure 12, the graph derived from simulation employing a single-phase methodology demonstrates a linear augmentation. Similarly, the graph produced from the multiphase methodology reflects a somewhat linear increase up to the Reynolds number of 3000. Subsequently, the slope experiences a notable decline in comparison to the slope of the graph acquired from the single-phase methodology. This phenomenon can be attributed to the fact that, prior to reaching a Reynolds number of 3000, the enhancement in heat transfer characteristics due to the intermixing of the fluid and nanoparticles appears to exert a predominant influence. Beyond a Reynolds number of 3000, the additional mixing seems to exert a diminished impact on the Nusselt number, as the enhancement of heat transfer resulting from mixing gradually approaches its maximum threshold, thereby causing the slope to decrease. For identical Reynolds numbers,

the single-phase methodology exhibits a superior Nusselt number.

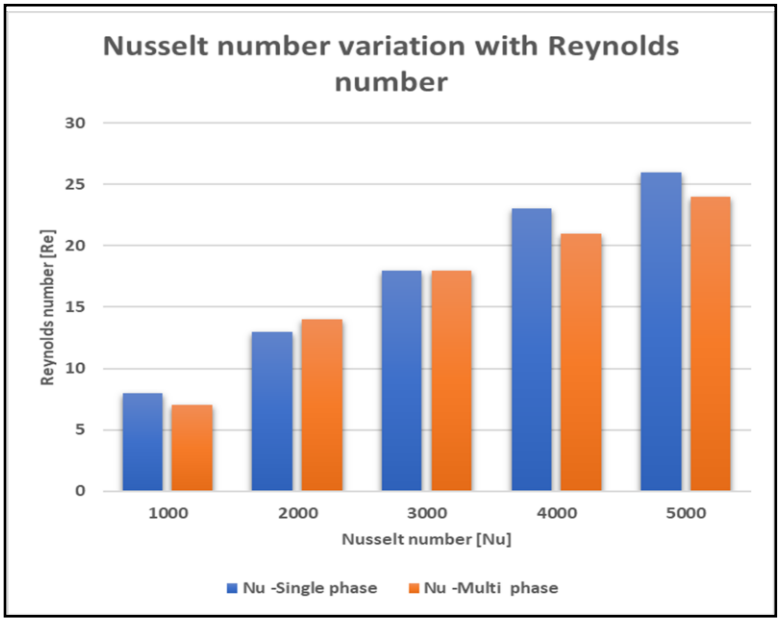

Figure 6: Nusselt number variation with Reynolds number

3.4 Effect on Surface Heat Transfer Coefficient

The influence of the Reynolds number on the surface heat transfer coefficient exhibits a resemblance to that of the Nusselt number.

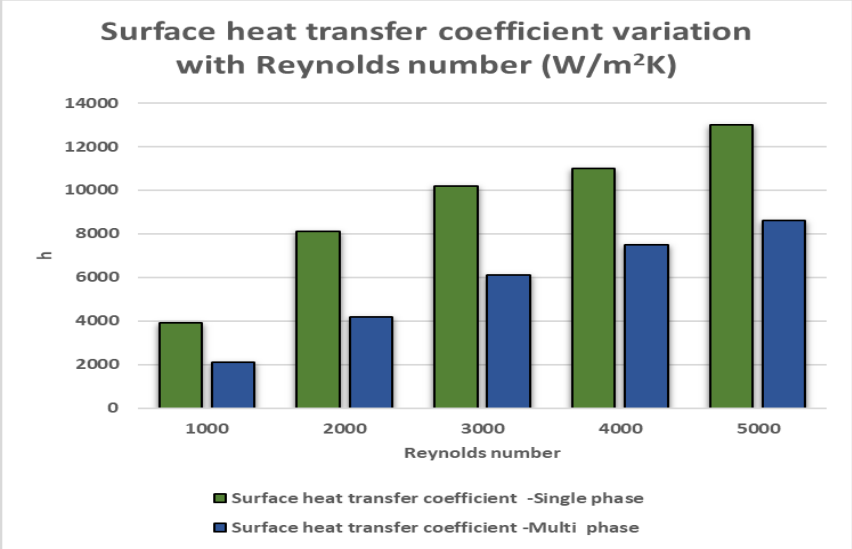

Figure 7: Surface heat transfer coefficient variation with Reynolds number (W/m^2K)

Figure 7 illustrates a linear increase in the surface heat transfer coefficient in relation to the Reynolds number within the single-phase framework. In the multiphase framework, the surface heat transfer coefficient exhibits a nearly linear escalation up to a Reynolds number of 2500, after which the incline diminishes, yet the correlation remains predominantly linear.

As the Reynolds number associated with the fluid flow escalates, the propensity for turbulence within the nanofluids also intensifies. This phenomenon facilitates the intermingling of substantial volumes of fluid that engage in vigorous heat exchange. Consequently, this enhancement augments the rate of heat transfer both within the fluid itself and through the boundary of the fluid domain to the external environment. As a result of this occurrence, both the surface heat transfer coefficient and the Nusselt number experience an increase.

3.5 Effect on Skin Friction Coefficient

At a fixed Reynolds number, an increase in the volume fraction of nanoparticles corresponds with a concomitant rise in skin friction, as previously elucidated. In order to investigate the impact of variations in Reynolds number on the skin friction coefficient of nanofluids, simulations were executed at a constant volume fraction of 5% and a steady inlet temperature of 363 K, employing both single-phase and multiphase methodologies.

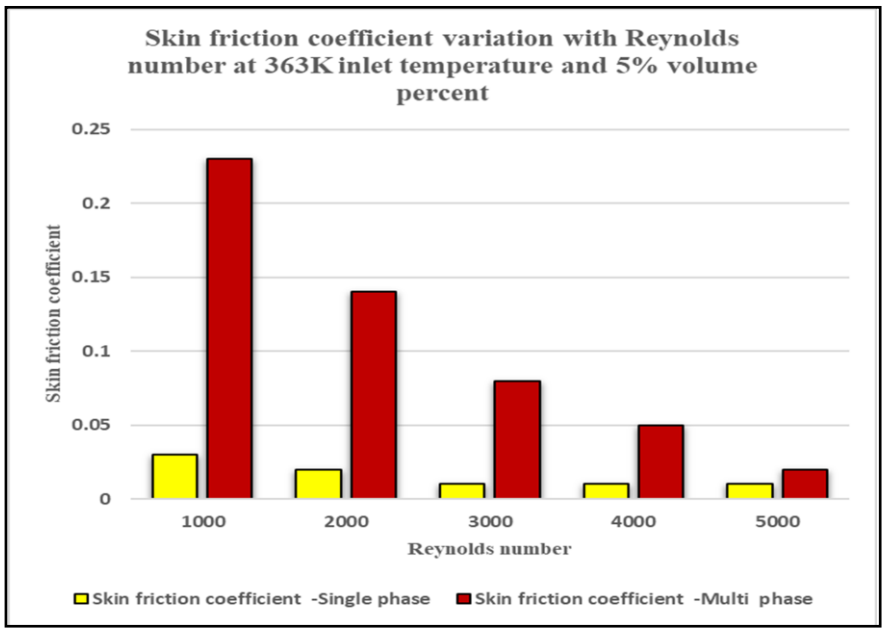

Figure 8: Skin friction coefficient variation with Reynolds number at 363K inlet temperature and 5% volume percent

As delineated in figure 14, the mean skin friction coefficient exhibits a decrement with the augmentation of the Reynolds number. This reduction is attributable to the diminishing influence of viscous forces on skin friction as the Reynolds number escalates. The single-phase simulation reveals a lower magnitude of skin friction coefficient in comparison to that observed in the

multiphase simulation. The impact of the skin friction coefficient in relation to the Reynolds

number is less pronounced in the single-phase simulation than in the multiphase simulation due to the absence of actual nanoparticles and their interactions with the base fluid as well as with other nanoparticles within the single-phase context. Consequently, for a fixed volume fraction, skin friction experiences a decline concomitant with an increase in fluid velocity.

3.6 Effect of Volume Fraction

3.6.1 Effect on Nusselt Number

The volumetric ratio of the nanoparticles was systematically adjusted from 0.5% to 5%. The resultant Nusselt number was determined and juxtaposed with that of the base fluid through the graphical representation of the ratio of the Nusselt number of nanofluids to that of the base fluid, in conjunction with the variations in the volumetric ratio of the nanoparticles. Both single-phase and multiphase computational simulations were executed by modifying the volumetric ratio, and the subsequent curves obtained are depicted in Figure 15.

Figure 14 illustrates that the ratio, Nunf/Nubf, exhibits a linear increase with the augmentation of the volumetric ratio in the context of the single-phase simulation. The elevation in the Nusselt number is markedly more pronounced in the multiphase simulation compared to the single-phase simulation. For volumetric ratios ranging from 0.1% to 1%, the multiphase simulation yielded a Nusselt number that was 5-45% superior to that of the single-phase simulation, which aligns with the findings reported by Delvari et al. [5], indicating a 10-45% increase for volumetric ratios up to 1%. For volumetric ratios exceeding 1%, the multiphase simulation achieved an even greater Nusselt number; however, beyond a volumetric ratio of 3%, further augmentation of the volumetric ratio does not yield a significant increase in the Nusselt number. Therefore, augmenting the volumetric

ratio past a certain threshold does not invariably lead to an elevation in the Nusselt number, and an optimal result can be realized at approximately 2-2.5% volumetric ratio, where the Nusselt number derived from the multiphase simulation is roughly 1.7 times greater than that obtained from the single-phase simulation.

The increase observed in the Nusselt number of nanofluids is approximately 1.6 times that of the base fluid at a volumetric ratio of 5% and continues to escalate linearly as documented in the pertinent literature.

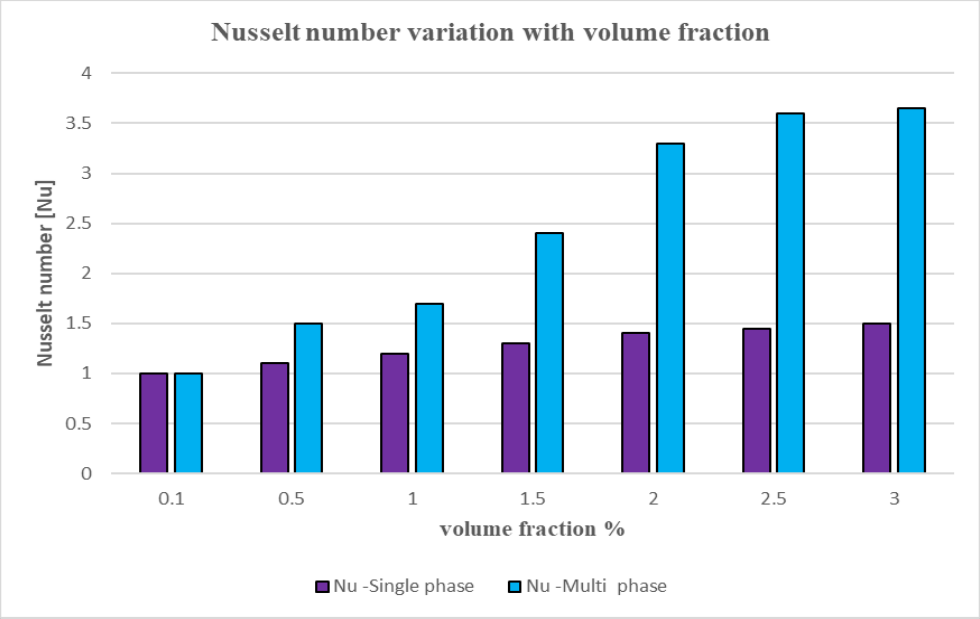

Figure 9: Nusselt number variation with volume fraction

Conversely, the outcomes derived from the Eulerian multiphase simulation indicate a substantial enhancement in the Nusselt number. In contrast to single-phase simulation, this alteration is characterized by non-linearity. The ratio exhibits an increase up to a 3% volume fraction, subsequent to which it stabilizes. It achieves a peak value of approximately 3.5 at around a 3% volume fraction.

3.6.2 Effect on Friction Coefficient, Pressure Loss and Pumping Power:

Figure 16a illustrates that the coefficient of skin friction exhibits an upward trend concomitant with the increasing volume fraction of nanoparticles. This augmentation in the skin friction coefficient exerts a significant effect on the pressure drop as well as the requisite pumping power, which are delineated by equations 22 and 23, respectively. As evidenced in figures 16a and 16b, both the single-phase and multiphase simulations yield analogous results. With the escalation of the volume fraction, the skin friction coefficient escalates, consequently leading to a substantial rise in the pressure drop. Consequently, there is an increase in the required pumping power.

The volume fraction demonstrates a nearly identical influence on the skin friction coefficient, pressure drop, and pumping power for both single-phase and multiphase simulations.

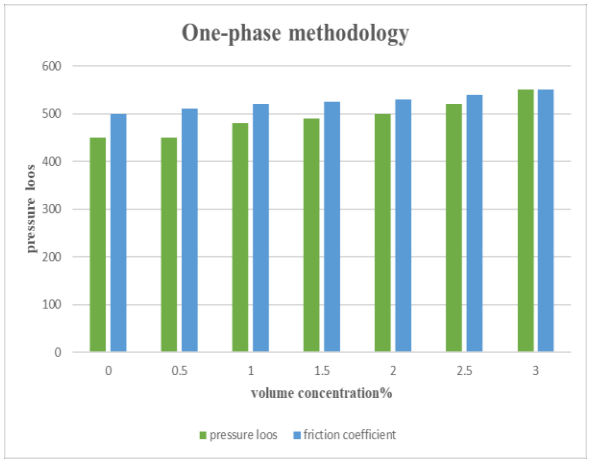

a. One-phase methodology

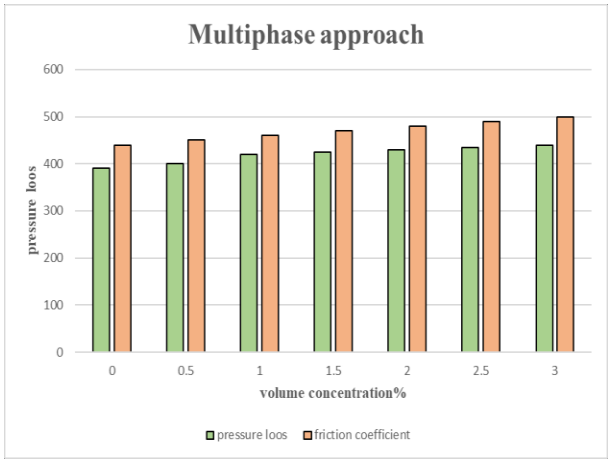

b. Multiphase approach

Figure 10: Changes in skin friction coefficient, pumping power, and pressure drop with volume fraction

The multiphase simulation exhibited a marginally reduced pumping power in comparison to the single-phase simulation. This phenomenon can be attributed to the elevated Reynolds number

associated with the multiphase simulation, given the identical inlet velocity and volume fraction, as the empirical correlation utilized for the viscosity calculation of the nanofluid yields a viscosity value that surpasses that obtained from the multiphase simulation. As illustrated in Figure 14, an augmentation in the Reynolds number precipitates a reduction in the skin friction coefficient, consequently leading to diminished pressure loss and pumping power.

3.6.3 Effect of Inlet Temperature

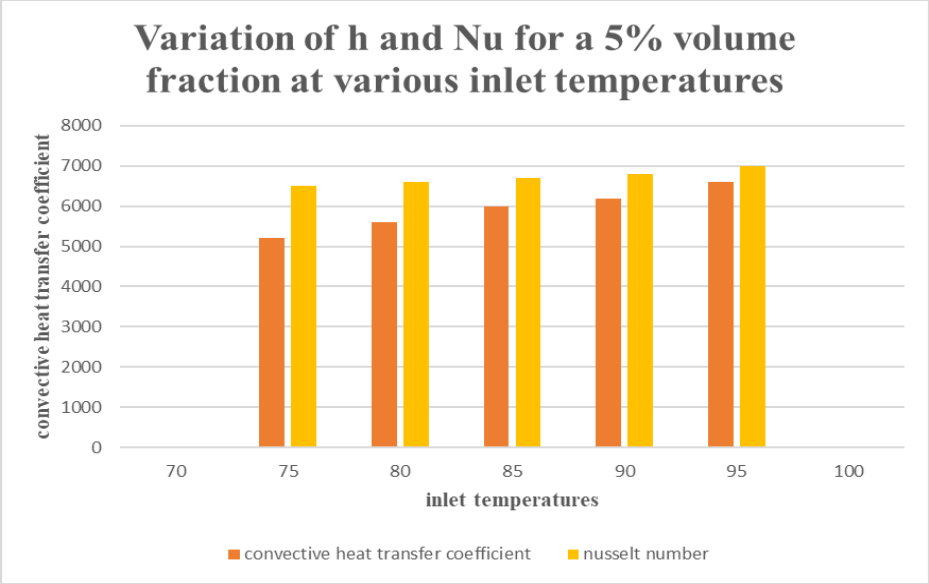

Figure 11: Variation of h and Nu for a 5% volume fraction at various inlet temperatures

To ascertain the impact of the inlet fluid temperature on the surface heat transfer coefficient, the simulation was conducted within a thermal range of 75°C to 95°C, which represents a typical temperature that a coolant achieves within a vehicular cooling system. The inlet temperature was systematically altered while maintaining a constant volume fraction of the nanoparticle at 5%, a

consistent inlet fluid velocity of 0.9 m/s, and a nanoparticle diameter of 25 nm.

The graphical representation in figure 17 illustrates the correlation between the surface heat transfer coefficient and the Nusselt number with respect to the inlet fluid temperature. Both parameters exhibit a linear increase in response to rising inlet temperatures. However, the magnitude of this variation is not as pronounced as observed in the Reynolds number discussed in subsection 3.4. Consequently, the escalation in inlet temperatures exerts a marginally lesser influence on both the surface heat transfer coefficient and the Nusselt number.

3.7 Effect of Particle Size

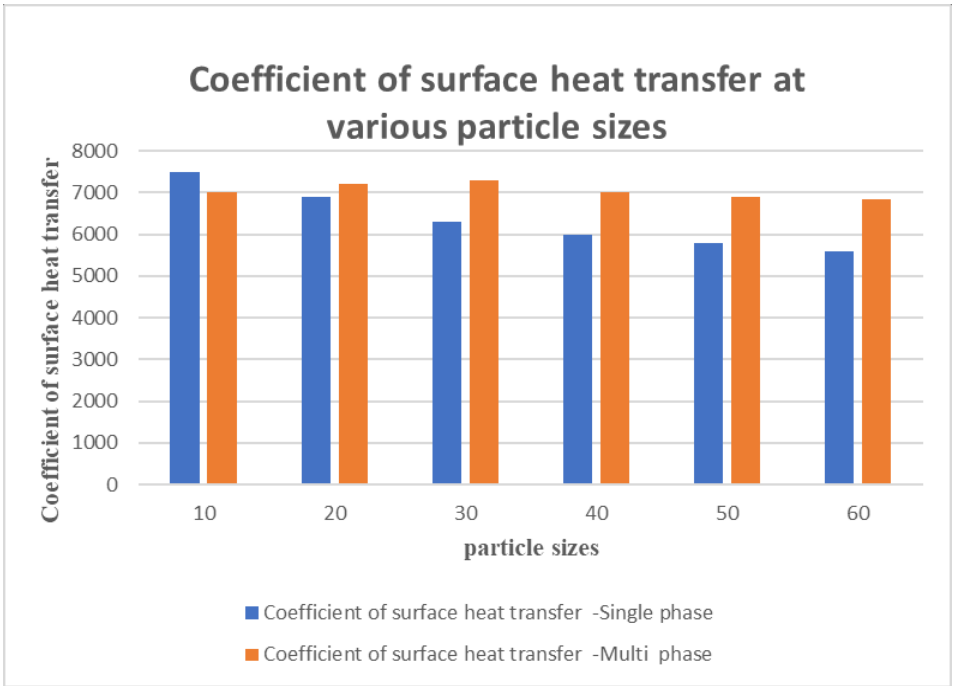

Figure 12: Coefficient of surface heat transfer at various particle sizes

To investigate the influence of varying nanoparticle dimensions, both single-phase and multiphase methodologies were examined. The simulation employing a single-phase methodology, as depicted in figure 18, indicates that an increase in particle size correlates with a

reduction in the surface heat transfer coefficient, implying that both the effective surface area and the frequency of collisions diminish as particle dimensions increase.

The findings from the multiphase methodology demonstrate that the surface heat transfer coefficient diminishes upon increasing the particle size from 25 nm to 60 nm. Likewise, for particle sizes below 25 nm, a decline in the heat transfer coefficient is observed. For nanoparticle sizes under 25 nm, the phenomenon of agglomeration appears to exert a more pronounced influence on heat transfer characteristics than does the enhancement of effective surface area.

4. Conclusion and Future Work

CFD analysis was performed on Cu2O3 and Propylene Glycol/water-based nanofluids utilizing both single-phase and multiphase methodologies to investigate the thermal performance of nanofluids within a flat tube of an automotive radiator. Various parameters, including inlet temperature, inlet velocity, nanoparticle volume concentration, and nanoparticle size, were systematically altered to assess the variations in heat transfer performance relative to base fluids. Of the two simulation approaches employed, the multiphase method yielded results that were more congruent with existing literature. Adjustments in the volume fraction of Cu2O3 nanoparticles, spanning from 0.5% to 5%, indicated that the heat transfer rate reached its peak at a 3% volume fraction, as evidenced by the corresponding peak in the Nusselt number at this concentration, which was three times greater than that observed in the base fluid. The modification of the Reynolds number demonstrated a linear increase in both the Nusselt number and the surface heat transfer coefficient across laminar and turbulent flow conditions; however, the increase was less pronounced within the turbulent regime. An escalation in nanoparticle volume concentration resulted in a marginal rise in skin friction, pressure drop, and the pumping

power requisite; nevertheless, the increase in power was minimal in contrast to the significant enhancement in heat transfer capability associated with elevated volume fractions. Correspondingly, a single-phase investigation examining the variation in inlet temperatures from 75°C to 95°C—within the typical operational temperature range for automotive radiators—also revealed an increase in both the Nusselt number and the heat transfer coefficient. Yet, this increment was insignificant when juxtaposed with the variations induced by changes in volume concentration, which represent a more manageable parameter than inlet temperature. In a similar vein, the multiphase analysis encompassing nanoparticle sizes ranging from 10 nm to 60 nm indicated optimal thermal performance at a nanoparticle size of 25 nm, revealing a gradual reduction in the heat transfer coefficient as particle size increased or decreased beyond the 25 nm threshold. Notably, superior performance was observed at a particle size of 25 nm.

While the single-phase approach offers advantages in terms of computational efficiency, energy consumption, and time savings, it is imperative that multiphase simulations be more frequently employed to enhance the predictive accuracy of nanofluid behavior. This investigation was constrained by limited computational resources, necessitating steady-state simulations. It is recommended that transient simulations be conducted in subsequent studies to yield more precise and realistic outcomes, incorporating genuine turbulent phenomena and accurate phase interactions. The current study was confined to a single tube within a radiator, operating under the assumption that heat loss occurred uniformly from the tube wall at a constant rate. However, an analysis incorporating both fins and tubes through conjugate heat transfer methodology could potentially provide more realistic results and is recommended for future investigations.

References

1. Mazaheri, Nima, and Mehdi Bahiraei. "Performance enhancement of a photovoltaic

thermal system through two-phase nanofluid simulation in a channel equipped with novel artificial roughness." Applied Thermal Engineering 230 (2023): 120709.

2. Thabit, Saif M., and Waleed M. Abed. "Experimental and Numerical Convective Heat Transfer Investigation in Laminar Rectangular-Channel Flow across V-Shaped Grooves." Journal of Enhanced Heat Transfer 30, no. 2 (2023).

3. Rijvi, Fahim Rahaman, and Mohammad Sultan Mahmud. "Enhancing the Thermal Performance of Radiators using Nanofluids-A CFD Approach."

4. Choi, S. U. S., and Jeffrey A. Eastman. "Enhancing thermal conductivity of fluids with nanoparticles, Argonne National Lab.(ANL), Argonne, IL (United States), 1995." (2022).

5. Delavari V, Hashemabadi SH, 2014, "CFD simulation of heat transfer enhancement of Cu_2O_3/water and Cu_2O_3/Propylene Glycol nanofluids in a car radiator," *Applied Thermal Engineering*, 73, pp. 380-390.

6. Maghrabie, Hussein M., and Hamouda M. Mousa. "Thermal performance intensification of car radiator using SiO2/water and ZnO/water nanofluids." Journal of Thermal Science and Engineering Applications 14, no. 3 (2022): 034501.

7. Chandrasekar M, Suresh S, Chandra Bose A., 2010, " Experimental investigations and theoretical determination of thermal conductivity and viscosity of Cu2O3/water nanofluids," *Experimental Thermal and Fluid Science*, 34, pp. 210-216.

8. Peyghambarzadeh SM, Hashemabadi SH, Hoseini SM, Seifi Jamnani M., 2011, " Experimental study of heat transfer enhancement using water/Propylene Glycol based nanofluids as a new coolant for car radiators," *International Communications in Heat and Mass Transfer*, 38, pp. 1283-1290.

9. Pooyoo, Narong, and Sivanappan Kumar. "Numerical Simulation of Cylindrical Heat

Pipe Using Al2O3-Water Nanofluid as the Working Fluid." International Energy Journal 22, no. 3 (2022).

10. Ghimire, Rahul, Pankaj Mehta, Nischal Aryal, Daya Ram Sah, and Surya Prasad Adhikari. "Thermal Performance of Car Radiator Operated by Al_2O_3–Ethylene Glycol/Water-Based Nanofluids: A Computational Fluid Dynamics Study." Journal of Thermal Science and Engineering Applications 15, no. 1 (2023): 011012.

11. Keshavarz Moraveji M, Razvarz S., 2012, "Experimental investigation of aluminum oxide nanofluids on heat pipe thermal performance," I*nternational Communications in Heat and Mass Transfer*, 39, pp. 1444-1448.

12. Gürdal, Mehmet, Hayati Kadir Pazarlıoğlu, Mutlu Tekir, Kamil Arslan, Engin Gedik, and Edip Taşkesen. "Experimental investigation on thermo hydraulic performance of ferronanofluid flow in a dimpled tube under magnetic field effect." Experimental Heat Transfer 36, no. 3 (2023): 312-330.

13. Zhao, N., Yang, J., Li, H., Zhang, Z., Li, S., 2016, "Numerical investigations of laminar heat transfer and flow performance of Cu2O3-water nanofluids in a flat tube" *Int. J. Heat Mass Transfer*, 92, pp. 268–282.

14. Najım, Saad, Adnan Husseın, and Suad Hassan Danook. "Performance improvement of shell and tube heat exchanger by using Fe3O4/water nanofluid." Journal of Thermal Engineering 9, no. 1 (2023): 24-32.

15. McQuiston, Faye C., Jerald D. Parker, Jeffrey D. Spitler, and Hessam Taherian. Heating, ventilating, and air conditioning: analysis and design. John Wiley & Sons, 2023.

16. Akhatov, J. S., T. I. Juraev, and T. D. Juraev. "Comparison of different empirical models for analysing the thermal conductivities of various materials for use in nanofluid

preparation." Applied Solar Energy 58, no. 1 (2022): 76-85.

17. Sujith, Surendran V., Hansoo Kim, and Joonho Lee. "A review on thermophysical property assessment of metal oxide-based nanofluids: industrial perspectives." Metals 12, no. 1 (2022): 165.

18. Avramenko, Andriy A., and Igor V. Shevchuk. Modelling of convective heat and mass transfer in nanofluids with and without boiling and condensation. Springer Nature, 2022.

19. Canbolat, Ahmet Serhan, Ali Husnu Bademlioglu, and Omer Kaynakli. "Thermohydraulic Performance Optimization of Automobile Radiators Using Statistical Approaches." Journal of Thermal Science and Engineering Applications 14, no. 5 (2022): 051014.

20. Srinivasa Rao, Gurrala. "CFD Analysis of Afterburner with Convergent–Divergent Nozzle for Various Air–Fuel Ratios." In Conference on Fluid Mechanics and Fluid Power, pp. 253-267. Singapore: Springer Nature Singapore, 2022.

21. Ramadhan, Anwar Ilmar, Wan Hamzah Azmi, Rizalman Mamat, Ery Diniardi, and Tri Yuni Hendrawati. "Experimental investigation of cooling performance in automotive radiator using Al_2O_3-TiO_2-SiO_2 nanofluids." Automotive Experiences 5, no. 1 (2022): 28-39.

22. Upadhyay, Satish. "On the assessment of nano-oils for medium-temperature solar thermal systems." (2023).